

# A Direct Image of the Obscuring Disk Surrounding the Active Galactic Nucleus of NGC 1068

Jack F. Gallimore

*Max-Planck-Institut für extraterrestrische Physik,  
Postfach 1603, D-85740 Garching b. München, Germany,*

Stefi A. Baum and Christopher P. O'Dea

*Space Telescope Science Institute,  
3700 San Martin Dr., Baltimore, MD 21218, USA*

June 10, 2022

Active galactic nuclei (AGNs) are commonly thought to be powered by the exchange of gravitational energy for thermal energy in a compact accretion disk surrounding a massive black hole [1, 2]. Such disks are also necessary to collimate powerful radio jets [3]. The unifying schemes for AGN classification further propose that gas fuelling the AGN may obstruct our sight-line, hiding some AGNs from direct view; the popular model is a parsec-scale ( $1 \text{ pc} = 10^{18.5} \text{ cm}$ ) disk of dense molecular gas [4]. Evidence for such disks has been mostly indirect, since the angular size is much smaller than the resolution of conventional telescopes. We report the first direct images of a pc-scale disk of ionised gas located within the nucleus of NGC 1068, the archetype of obscured AGNs. The disk is viewed nearly edge-on, and individual clouds within the ionised disk are opaque to high-energy radiation, consistent with the unifying schemes model. In projection, the disk and AGN axes align, and so the ionised gas disk may be considered to trace the outer regions of the long-sought accretion disk.

The nucleus of the galaxy NGC 1068 hosts the archetypal example of an obscured AGN. The popular model for the obscuring medium is a parsec-scale, molecular disk surrounding the AGN [5], perhaps ultimately feeding an accretion disk [6, 7]. One difficulty for observational tests has been that the location of the obscured, central ionising source is unknown. It has been argued on several grounds that the radio source S1 marks the location of the hidden AGN in NGC 1068 [8, 9]. Located at the southern end of the arcsecond-scale radio jet, S1 is an unusual radio source in two respects. Firstly, in contrast with the rest of the radio jet, its radio spectrum is relatively flat (spectral index  $\alpha = +0.3$ ;  $S_\nu \propto \nu^\alpha$  [8]), and secondly, it is a source of H<sub>2</sub>O and OH maser emission [10], which distinguishes regions of peculiarly warm (1000 K) and dense ( $\gtrsim 10^8 \text{ molecules cm}^{-3}$ ) molecular gas. We argued that

S1 might trace emission from molecular clouds defining the inner surface of the proposed obscuring disk, whose surfaces would be exposed directly to the central X-ray source and are therefore hot and highly ionised [8].

There are two main predictions for the high resolution observations presented here. The obvious prediction is that S1 should resolve into a pc-scale, linear radio structure, tracing the profile of an edge-on disk or ‘torus’ projected onto the sky, and located within the warm, molecular disk mapped in part by H<sub>2</sub>O masers [10]. Secondly, the mean surface brightness of S1, in temperature units corresponding to an equivalent blackbody radiator (brightness temperature), should be  $T_b \sim 10^6$  K for scattering-diffused emission or thermal free-free emission [8].

To test these predictions, we have imaged the subarcsecond jet of NGC 1068 using the 10-station Very Large Baseline Array (VLBA), augmented by the phased, 26-element Very Large Array (VLA). The new images are displayed in Fig. 1. A single, deep (8.8 hrs on-source) integration was obtained at 8.4 GHz only. The observations and data reduction followed standard techniques with exceptions as follows. On continental-scale baselines, NGC 1068 is not sufficiently bright at 8 GHz to calibrate interferometric fringes within averaging times comparable to the atmospheric coherence time. Instead, we measured fringe-rate and -delay corrections from short scans of the nearby calibrator source 0237–027. Less than 0.2% of the data (one out of a total of nearly 600 baseline-hours) were affected by phase rotations resulting from fringe solution ambiguities, and the radio sources S1, C, and NE were clearly detected on the initial maps. The resulting, fringe-calibrated data were coherent over sufficiently long intervals to permit self-calibration, and so we removed the residual phase wraps using five iterations of phase-only self-calibration. In order to focus specifically on the nuclear emission, the VLBA images of NE and C will be presented elsewhere. We focus instead on the ‘Hot Zone’ (HZ), the brighter, central region of S1, and also defer discussion of fainter radio emission to future work.

The HZ comprises nine distinguishable compact sources, each of total flux density  $S_\nu \lesssim 0.65$  mJy ( $1 \text{ mJy} = 10^{-26} \text{ ergs s}^{-1} \text{ cm}^{-2} \text{ Hz}^{-1}$ ), embedded in diffuse emission. These observations only marginally resolve the individual compact sources. Based on Gaussian model fits and image moment analysis, the deconvolved source sizes are typically  $\sim 1$  milliarcsecond (mas), or  $\sim 0.07$  pc at the distance of NGC 1068. These measurements are however uncertain owing to confusion between neighboring sources, blurring due to residual phase errors, and possible enhancement by deconvolution. We also estimated limits on the source sizes based on inspection of the interference fringes. Less than half ( $\sim 3$  mJy) of the recovered flux of the HZ is detected on baselines corresponding to angular sizes  $< 2 \times 1$  mas; at least half of the flux from the HZ must therefore arise from structures  $\gtrsim 1$  mas in size, consistent with measurements of the synthesized image. This limit is conservative, since 1–2 mJy worth of mas-scale components are also detected towards components NE and C. Any one or two of these compact sources may be smaller than 1 mas, but this caveat will not affect the main conclusions.

The compact sources trace a slightly curving line along a position angle of  $110^\circ$ , measured east of north. The HZ is therefore nearly at right angles with the collimation axes defined by the local radio jet and polarisation axes, the latter of which describes the collimation axis for escaping ionising radiation [13]. This geometry is fully consistent with our prediction that the radio emission from S1 traces emission not from a streaming jet but rather from gas in an ionised disk surrounding the AGN. We next consider the implications of this disk model, making the simplifying assumption that the HZ gas lies at a common radius,  $\sim 0.3$ – $0.5$  pc, from the AGN.

Opaque synchrotron emission is the conventional explanation for flat-spectrum radio sources, but the brightness temperatures over the HZ are too low for synchrotron self-absorption [14]. There are two likely alternatives, illustrated in Fig. 2,

either being a variation on emission from ionised gas in a disk [8]. The first is synchrotron emission from a synchrotron-opaque, compact radio source, presumably the AGN, which is not viewed directly but in reflection by electron-scattering from the ionised gas disk.

The limits for this model are set by requiring that the electron scattering opacity ( $\tau_e$ ) must exceed the opacity to free-free absorption ( $\tau_{ff}$ ), and that the hidden radio source must not be so luminous that it would have been detected in reflection on larger scales. The limits for this model are set by requiring that the electron scattering opacity ( $\tau_e$ ) must exceed the opacity to free-free absorption ( $\tau_{ff}$ ), and that the hidden radio source must not be so luminous that it would have been detected in reflection on larger scales. Based on the sensitivities of our radio continuum images [8] and the reflecting properties of the electron-scattering mirror [15], we estimate that the hidden radio source can be no brighter than  $S_\bullet \lesssim 3.5$  Jy. We estimated limits on the plasma properties by exploring a grid of  $n_e$ ,  $T_e$ , and cloud thicknesses  $l$  (and the corresponding value  $S_\bullet$  appropriate for a given  $\tau_e$ ) and rejecting those values where  $\tau_{ff} > 0.5\tau_e$  and  $S_\bullet > 3.5$  Jy. We find that the reflection model can be satisfied for electron temperatures  $T_e \gtrsim 10^{6.7}$  K, electron densities  $10^{6.2} \lesssim n_e < 10^{6.6}$  electrons  $\text{cm}^{-3}$ , and ionised cloud thicknesses  $0.007 \lesssim l \lesssim 0.07$  pc (the upper limit set by the measured sizes). We also estimate that, assuming that thermal absorption is negligible, the flux density of any hidden compact radio source must be  $0.8 \lesssim S_\bullet \lesssim 3.5$  Jy.

The second model is direct, thermal free-free emission from ionised gas inside the obscuring disk. Appropriate for the integrated radio spectrum [9, 11], we assume for this thermal model a mean opacity of  $\tau_{ff}(8.4 \text{ GHz}) = 0.5$  through the Hot Zone plasma. Using the free-free opacity approximations of Mezger and Henderson [16], we estimate  $10^{6.5} \lesssim T_e \lesssim 10^{6.8}$  K and  $n_e \gtrsim 10^{6.8} \text{ cm}^{-3} (T_e/10^7 \text{ K})^{1.35} (l/0.07 \text{ pc})^{0.5}$ .

The plasma conditions in either the thermal or reflection models are plausible

given the extreme environment. For comparison, particle densities in the molecular region of the disk are estimated to be  $n_{H_2} \approx 10^8$  molecules  $\text{cm}^{-3}$  [7, 17], and photoionisation heating can drive  $T_e$  up to the limit bound by inverse Compton cooling,  $T_C \sim 10^7$ – $10^8$  K [7, 18]. On the other hand, it is not clear how such a dense medium can remain heated to temperatures so near the Compton limit. For instance, photoionisation heating of dense plasmas can support only  $T_{cool} \sim 10^4$ – $10^6$  K [7, 19], unless the ionising spectrum is much harder (more luminous in X-rays) and overall more luminous than current estimates [20]. A promising alternative is heating by mixing with a hot, intercloud medium [21], a  $T_{hot} \sim 10^7$ – $10^8$  K plasma proposed to confine optical emission line clouds in the nuclear environment [18]. The temperatures in the mixed plasma would be  $T_e \approx \sqrt{T_{cool}T_{hot}}$  [22], or  $T_e \sim 10^{6.5}$  K, to within factors of a few. In addition, fast shocks, such as those driven by winds or the radio jet, or internal shocks arising at cloud-cloud collisions, might at least transiently support such high temperatures. Understanding the energy budget of the HZ will be a challenge for follow-up research.

Relevant specifically to AGN unifying schemes, the column density through the HZ clouds may be as high as  $n_{el} \sim 10^{24}$   $\text{cm}^{-2}$ , sufficient to absorb virtually all of the incident X-ray emission from the AGN [23]. This result and that the disk is viewed nearly edge-on argue that the HZ traces ionised gas lying within the obscuring disk of NGC 1068. One difficulty is that the covering fraction of the compact sources,  $\sim 5$ – $10\%$ , is much smaller than required generally to explain the fraction of directly viewed AGNs [24]. However, the model can be reconciled if the geometric thickness of the obscuring medium increases with radius [25], and the HZ traces only emission from disc material nearest the AGN. Alternatively, the obscuring disk might instead be thin but highly warped [26], and again the HZ marks only the centermost region of the disk.

Turning to the broad-band properties of the disk, the HZ plasma must also

be a source of line and continuum emission up to soft X-ray energies. To determine whether the optical–X-ray spectrum of the HZ might be distinguished from neighboring emission line regions and the AGN proper, we modelled the HZ spectrum using the CLOUDY photoionisation code [27], programmed to emulate a cooling plasma with the properties of the HZ, and normalised to the observed radio flux. We find that, in broad agreement with Pier and Voit [7], the HZ contributes  $\lesssim 10\%$  to the observed optical–UV emission lines of NGC 1068 and  $\lesssim 1\%$  to the optical–UV continuum. On the other hand, the HZ should contribute significantly to the soft X-ray spectrum of the nucleus were the AGN viewed along an unobscured sight-line. We estimate that free-free emission from the HZ may contribute  $\gtrsim 10\%$  of the AGN continuum in soft X-rays (photon energies  $\sim 1\text{--}2$  keV). Moreover, the predicted soft X-ray line emission exceeds that observed toward NGC 1068 [28] by a factor of  $\gtrsim 100$ . This observed diminution is approximately that expected for *obscured* X-ray emission viewed only in reflection [20]. Therefore, this result can be reconciled if the HZ is also heavily obscured over optical–soft X-ray wavebands. The implication is that, if the AGN unifying schemes hold generally, the disks surrounding unobscured AGNs should be luminous soft X-ray emission line sources. To our knowledge, there has as yet been no analysis of the soft X-ray line emission from unobscured AGNs (i.e., Seyfert 1 AGNs). The detection of soft X-ray lines characteristic of a  $10^6\text{--}10^7$  K plasma in unobscured AGNs would lend self-consistency to the obscuring disk model.

The present observation is the first direct image of a pc-scale, ionised gas disk surrounding an AGN. Simple models for the radio emission further provide the first direct estimates of the physical properties of a pc-scale disk, and the results are consistent with the predictions of AGN unifying schemes. However, we also find that photoionisation heating is insufficient to support the high plasma temperatures in the disk, and so the challenge remains to model the energy budget in accord

with the observed radio emission. Equally important is how the HZ might fit into the standard, infall model for AGNs [2]. The HZ is oriented nearly at right angles to the radio jet. The observed orientation suggests that, within the HZ, internal, viscous dissipation drives the fueling of the AGN rather than external torques. In this regard, the HZ may be considered to define the outer extent of the long-sought accretion disk powering the AGN.

Correspondence and requests for materials to J.F.G. (e-mail: jfg@hethp.mpe-garching.mpg.de).

## References

- [1] Rees, M. J. Black hole models for active galactic nuclei. *Ann. Reviews Astron. Astrophys.* **22**, 471–506 (1984).
- [2] Gunn, J.E. Feeding the monster – Gas discs in elliptical galaxies. In *Active Galactic Nuclei*, (eds. C. Hazard & S. Mitton) 213-225 (Cambridge University Press, Cambridge, 1979).
- [3] Begelman, M.C., Blandford, R.D., & Rees, M. J. Theory of extragalactic radio sources. *Rev. Mod. Phys.* **56**, 255–351 (1984).
- [4] Lawrence, A. Classification of active galaxies and the prospect of a unified phenomenology. *Publ. Astron. Soc. Pacif.* **99**, 309–334 (1987)
- [5] Antonucci, R. R. J., & Miller J. S. Spectropolarimetry and the nature of NGC 1068. *Astrophys. J.* **297**, 621–532 (1985).
- [6] Krolik, J. H., & Begelman, M. C. Molecular tori in Seyfert galaxies - Feeding the monster and hiding it. *Astrophys. J.* **329**, 702–711 (1988).
- [7] Pier, E.A., & Voit, G.M. Photoevaporation of dusty clouds near active galactic nuclei. *Astronomy J.* **150**, 628–637 (1995)



- [8] Gallimore, J. F., Baum, S. A., & O’Dea, C. P. The subarcsecond radio structure in NGC 1068. II. Implications for the central engine and unifying schemes. *Astrophys. J.* **464**, 198–211 (1996).
- [9] Muxlow, T. W. B., Pedlar, A., Holloway, A. J., Gallimore, J. F., & Antonucci, R. R. J. The compact radio nucleus of the Seyfert galaxy NGC 1068. *Mon. Not. R. Astron. Soc.* **278**, 854–860 (1996).
- [10] Gallimore, J. F., Baum, S. A., O’Dea, C. P., Brinks, E., & Pedlar, A. H<sub>2</sub>O and OH masers as probes of the obscuring torus in NGC 1068. *Astrophys. J.* **462**, 740–745 (1996)
- [11] Gallimore, J. F., Baum, S. A., O’Dea, C. P., & Pedlar, A. The subarcsecond radio structure in NGC 1068. I. Observations and results. *Astrophys. J.* **458**, 136–148 (1996)
- [12] Cornwell, T., & Braun, R. Deconvolution. In *Synthesis Imaging in Radio Astronomy* (eds Perley, R.A., Schwab, F.R. & Bridle, A.H.) 167–181 (A.S.P. Conference Series, San Francisco, 1994).
- [13] Antonucci, R.R.J., Hurt, T., & Miller, J.S. HST ultraviolet spectropolarimetry of NGC 1068. *Astrophys. J.* **430**, 210–217 (1994)
- [14] Kellerman, K.I. & Owen, F. N. Radio galaxies and quasars. In *Galactic and Extragalactic Radio Astronomy* (eds Verschuur, G.L. & Kellermann, K.I.) 563–600 (Springer, New York, 1989)
- [15] Capetti, A., Macchetto, F., Axon, D.J., Sparks, W.B., & Boksenberg, A. Hubble Space Telescope imaging polarimetry of the inner nuclear region of NGC 1068. *Astrophys. J. Lett.* **452**, L87–L89 (1995).
- [16] Mezger, P.G., Henderson, A.P. Galactic H II regions: I. Observations of their continuum radiation at the frequency 5 GHz. *Astrophys. J.* **147**, 471–489 (1967)

- [17] Neufeld, D.A., Maloney, P.R., & Conger, S. Water maser emission from X-ray-heated circumnuclear gas in active galaxies *Astrophys. J. Lett.* **436**, L127–L130 (1994)
- [18] Krolik, J.H., McKee, C.F. & Tarter, C.B. Two-phase models of quasar emission line regions. *Astrophys. J.* **249**, 422–442 (1981)
- [19] Krolik, J.H., & Begelman, M.C. An X-ray heated wind in NGC 1068. *Astrophys. J. Lett.* **308**, L55–L58 (1986)
- [20] Pier, E. A., Antonucci, R., Hurt, T., Kriss, G., & Krolik, J. The intrinsic nuclear spectrum of NGC 1068. *Astrophys. J.* **428**, 124–129 (1994).
- [21] Reynolds, C.F. & Fabian, A.C. Warm absorbers in active galactic nuclei. *Mon. Not. R. Astron. Soc.* **273**, 1167–1176 (1995).
- [22] Begelman, M.C. & Fabian, A.C. Turbulent mixing layers in the interstellar and intracluster medium *Mon. Not. R. Astron. Soc.* **244**, 26P–29P.
- [23] Mulchaey, J. S., Mushotzky, R. F., & Weaver, K. A. Hard X-ray tests of the unified model for an ultraviolet-detected sample of Seyfert 2 galaxies. *Astrophys. J.* **390**, L69–L72 (1992).
- [24] Lawrence, A. The relative frequency of broad-lined and narrow-lined active galactic nuclei – Implications for unified schemes. *Mon. Not. R. Astron. Soc.* **252**, 586–592 (1991).
- [25] Efstathiou, A., Hough, J.H., & Young, S. A model for the infrared continuum spectrum of NGC 1068. *Mon. Not. R. Astron. Soc.* **277**, 1134–1144 (1995)
- [26] Sanders, D.B., Phinney, E.S., Neugebauer, G., Soifer, B.T., & Matthews, K. Continuum energy distribution of quasars – Shapes and origins. *Astrophys. J.* **257**, 29–51 (1986)

- [27] Ferland, G. *HAZY, a Brief Introduction to Cloudy*, University of Kentucky Physics and Astronomy Department Internal Report (1993)
- [28] Ueno, S., Mushotzky, R.F., Koyama, K., Iwasawa, K., Awaki, H., & Hayashi, I. ASCA observations of NGC 1068. *Publ. Astron. Soc. J.* **46** L71–L75 (1994)

**Acknowledgements.** The VLBA and VLA are operated by the National Radio Astronomy Observatory which is operated by Associated Universities, Inc., under cooperative agreement with the National Science Foundation. J.F.G. received support from a Collaborative Visitor’s Grant from the Space Telescope Science Institute. We also acknowledge useful suggestions from an anonymous referee which helped to clarify the text.

Figure 1: New VLBI images of the radio component S1 of NGC 1068. The total recovered flux of the HZ is 6.9 mJy, or roughly 60% of the flux anticipated by a power-law interpolation of the 5 GHz and 22 GHz measurements of Gallimore et al. [11]. In contrast, less than a total of  $\sim 1$  mJy arises from compact structures lying outside the Hot Zone (HZ) but within S1. Owing to an instability in the deconvolution algorithm used to produce this image, some of the compact sources may be artificially enhanced at the expense of the diffuse emission [12]. The compact sources are nevertheless real, since they are also distinguishable on the unprocessed images. *Upper plot:* Naturally weighted image of S1; the beam size (FWHM), indicated by the darkened ellipse, is  $2.5 \times 1.4$  mas. We have marked and labeled the HZ and the local jet axis towards radio jet component C. Note that, in projection, the extent of the HZ and the direction of the radio jet are at right angles to each other, suggesting a common symmetry axis. Scaled logarithmically, the contour levels are  $\pm 0.10$  ( $2.5\sigma$ ), 0.22, 0.35, 0.47, and 0.59 mJy beam $^{-1}$ , or  $\pm 0.49$ , 1.1, 1.7, 2.3, and 2.9 in brightness temperature units of  $10^6$  K. *Lower plot:* Uniformly weighted image of the HZ; the beam size (FWHM) is  $2.3 \times 1.1$  mas. The contour levels are  $\pm 0.16$  ( $2.5\sigma$ ), 0.24, 0.36, and 0.54 mJy beam $^{-1}$ , or  $\pm 1.1$ , 1.6, 2.5,  $3.7 \times 10^6$  K.

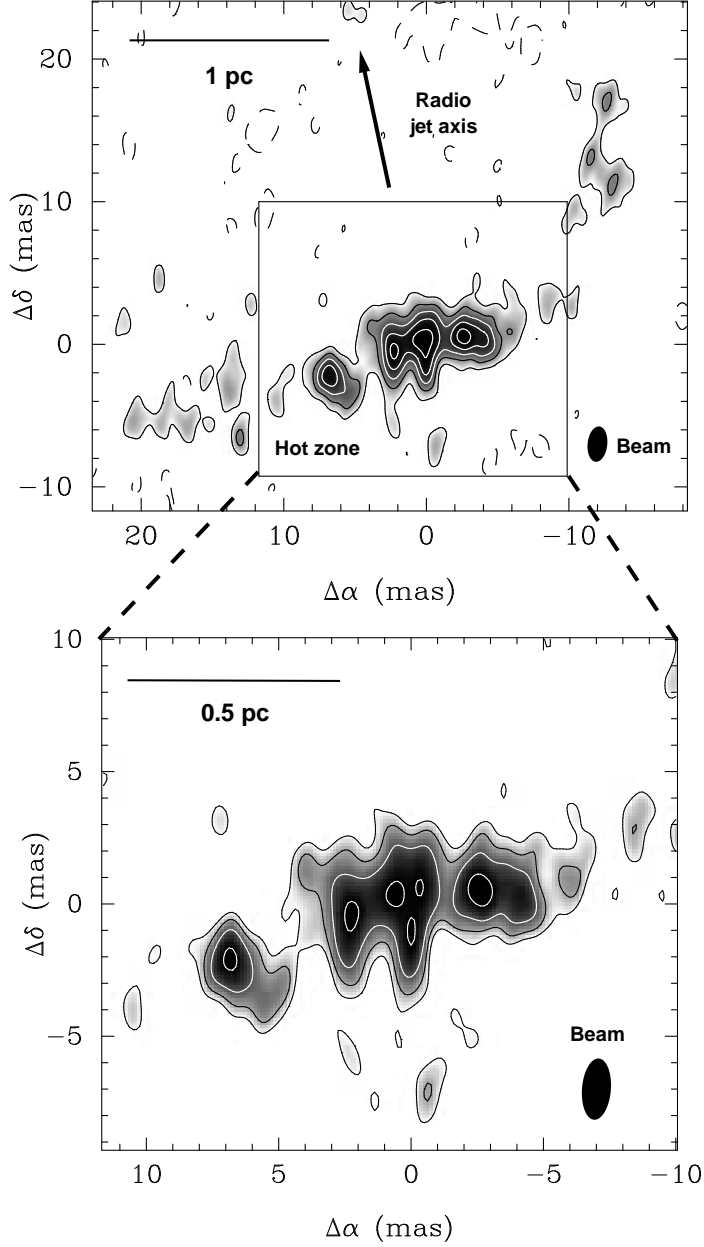


Figure 2: Model schematics of the AGN of NGC 1068 and its environs. *Left Panel:* A cartoon depicting the obscuring disk as viewed along our sight-line. The AGN is hidden from direct view, but we see reprocessed and scattered emission from the surrounding disk (illuminated material at the center of the cartoon). *Right Panel:* A plan view of the same, but which also illustrates the relative locations of the  $10^6$  K Hot Zone, detected in these observations, the warm transition zone, traced by  $\text{H}_2\text{O}$  maser emission and HI absorption [10], and an outer, cooler molecular zone, which still eludes direct detection. It has been argued that the innermost region may be filled with a hot ( $10^8$  K), intercloud medium [18], which might be a source of heat for the HZ. This cartoon also illustrates two possible contributions to the observed radio emission: (1) scattered non-thermal emission originating at the AGN and (2) direct free-free emission from the Hot Zone.

